AMERICAN SOCIETY FOR MICROBIOLOGY | Journal of Virology®

PATHOGENESIS AND IMMUNITY

Functional Perturbation of Mucosal Group 3 Innate Lymphoid and Natural Killer Cells in Simian-Human Immunodeficiency Virus/Simian Immunodeficiency Virus-Infected Infant Rhesus Macaques

Brady Hueber,[a] Alan D. Curtis II,[b] Kyle Kroll,[a] Valerie Varner,[a] Rhianna Jones,[a] Sachi Pathak,[b] Michelle Lifton,[a] Koen K. A. Van Rompay,[c,d] Kristina De Paris,[b] R. Keith Reeves[a,e]

[a]Center for Virology and Vaccine Research, Beth Israel Deaconess Medical Center, Harvard Medical School, Boston, Massachusetts, USA
[b]Department of Microbiology and Immunology and Center for AIDS Research, School of Medicine, University of North Carolina at Chapel Hill, Chapel Hill, North Carolina, USA
[c]Department of Pathology, Microbiology and Immunology, University of California, Davis, Davis, California, USA
[d]California National Primate Research Center, University of California, Davis, Davis, California, USA
[e]Ragon Institute of Massachusetts General Hospital, MIT, and Harvard, Cambridge, Massachusetts, USA

ABSTRACT Mother-to-child transmission of human immunodeficiency virus type 1 (HIV-1) via breastfeeding is responsible for nearly half of new infections of children with HIV. Although innate lymphoid cells (ILC) and natural killer (NK) cells are found throughout the oral mucosae, the effects of HIV/simian-human immunodeficiency virus (SHIV) in these tissues are largely unknown. To better understand the mechanics of postnatal transmission, we performed a comprehensive study of simian immunodeficiency virus (SIV)/SHIV-infected infant rhesus macaques (RM) and tracked changes in frequency, trafficking, and function of group 3 ILC (ILC3) and NK cells using polychromatic flow cytometry and cell stimulation assays in colon, tonsil, and oral lymph node samples. Infection led to a 3-fold depletion of ILC3 in the colon and an increase in the levels of NK cells in tonsils and oral lymph nodes. ILC3 and NK cells exhibited alterations in their trafficking repertoires as a result of infection, with increased expression of CD103 in colon NK cells and curtailment of CXCR3, and a significant decrease in $\alpha4\beta7$ expression in colon ILC3. SPICE analyses revealed that ILC3 and NK cells displayed distinct functional profiles by tissue in naive samples. Infection perturbed these profiles, with a nearly total loss of interleukin-22 (IL-22) production in the tonsil and colon; an increase in the levels of CD107a, gamma interferon (IFN-γ), and tumor necrosis factor alpha (TNF-α) from ILC3; and an increase in the levels of CD107a, macrophage inflammatory protein 1 beta (MIP-1β), and TNF-α from NK cells. Collectively, these data reveal that lentivirus infection alters the frequencies, receptor repertoires, and functions of innate cells in the oral and gut mucosa of infants. Further study will be required to delineate the full extent of the effect that these changes have on oral and gut homeostasis, SHIV/SIV pathogenesis, and oral opportunistic disease.

IMPORTANCE Vertical transmission of HIV from mother to child accounts for many of the new cases seen worldwide. There is currently no vaccine to mitigate this transmission, and there has been limited research on the effects that lentiviral infection has on the innate immune system in oral tissues of infected children. To fill this knowledge gap, our laboratory studied infant rhesus macaques to evaluate how acute SIV/SHIV infections impacted ILC3 and NK cells, which are immune cells critical for mucosal homeostasis and antimicrobial defense. Our data revealed that SIV/SHIV infection led to a depletion of ILC3 and an increase of NK cells and to a functional

Citation Hueber B, Curtis AD, II, Kroll K, Varner V, Jones R, Pathak S, Lifton M, Van Rompay KKA, De Paris K, Reeves RK. 2020. Functional perturbation of mucosal group 3 innate lymphoid and natural killer cells in simian-human immunodeficiency virus/simian immunodeficiency virus-infected infant rhesus macaques. J Virol 94:e01644-19. https://doi.org/10.1128/JVI.01644-19.

Editor Guido Silvestri, Emory University

Address correspondence to R. Keith Reeves, rreeves@bidmc.harvard.edu.

Received 25 September 2019
Accepted 30 November 2019
Accepted manuscript posted online 4 December 2019
Published 14 February 2020

shift from a homeostatic to a multifunctional proinflammatory state. Taking the results together, we describe how lentiviral infection perturbs the oral and gastrointestinal mucosae of infant macaques through alterations of resident innate immune cells giving rise to chronic inflammation and potentially exacerbating morbidity and mortality in children living with HIV.

KEYWORDS human immunodeficiency virus, innate immunity, innate lymphoid cell, natural killer cells, simian immunodeficiency virus

Mother-to-child transmission of human immunodeficiency virus type 1 (HIV-1) via breastfeeding is widely considered responsible for half of new infections of children with HIV (1), including approximately 180,000 newly infected infants in 2017 alone (2). As breastfeeding comes with a myriad of benefits and as advocating for formula feeding is not without its own hurdles and repercussions, understanding the interplay between the oral immune response and virus could play an important role in limiting transmission (3). The oral immune network is continually exposed to diverse commensal microbial communities, airborne allergens/antigens, and foods and must react accordingly (4). This dynamic environment requires tight orchestration between resident immune and epithelial cells to maintain a balance between successful immune surveillance and toleration of harmless antigens and commensals (5). HIV/simian immunodeficiency virus (SIV) infection disrupts this delicate balance, altering the immune cell frequencies and phenotypes and resulting in a more extensively proinflammatory environment prone to opportunistic diseases (6, 7).

NK cells represent a heterogeneous cell population and an integral part of the innate immune response against viral infections. NK cells mediate protection by rapidly killing infected cells and affecting the adaptive immune response through the secretion of cytokines (8). The rapid protection afforded by NK cells suggests a capacity to limit perinatal transmission from infected mother to newborn. *In vitro* experiments have demonstrated that, through the copious secretion of the CC chemokines CCL3, CCL4, and CCL5 (ligands for CCR5), NK cells are able to suppress entry of the virus into target cells by competitive inhibition (9). Studies in HIV-infected children have shown elevated expression of NK cell activating and stimulatory receptors (10, 11). NK cells are capable of performing potent cytolytic functions and secreting proinflammatory cytokines and represent a subset of group 1 innate lymphoid cells (ILC). ILC constitute a heterogenous population of innate immune cells. Although they lack somatic rearrangement of antigen receptors, the members of this diverse family of tissue-resident, transcriptionally poised effector lymphocytes are capable of rapidly responding to tissue damage-associated danger signals and microbially induced signals by producing cytokines that promote pathogen killing (12). Group 3 ILC (ILC3), a subset of the innate lymphoid cell family, play a critical role in the maintenance of tolerance and immune homeostasis in the gastrointestinal (GI) tract of mammals (13, 14). They are characterized by their expression of the transcriptional factor retinoic acid-related orphan receptor gamma isoform t (RORγt) and of aryl hydrocarbon receptor (AHR) and by their lack of machinery to directly sense microbial patterns (i.e., those associated with Toll-like receptors [TLR]) (14). ILC3 are able to rapidly respond to tissue damage-associated danger signals and microbe-induced signals via prolific cytokine secretion, especially secretion of interleukin-17 (IL-17) and IL-22 (13, 15). IL-22 plays critical roles in prevention of inappropriate immune responses to microbial and environmental antigens, which can most clearly be described in the maintenance of healthy host interactions with commensal bacteria at mucosal surfaces (15). IL-17 has been shown to synergize with IL-22 to augment production of microbial peptides (16).

ILC3's central role as healthy gut mediators can be knocked out of balance by a variety of factors, including genetic and environmental factors and, notably, viral infection (15). Previous studies showed that HIV/SIV infections in particular cause massive loss of ILC3 and drive disruptions of tolerance and intestinal barrier integrity (17, 18). HIV-1 infection is linked with translocation of commensal bacteria and break-

down of the epithelium, leading to systemic inflammation (15). In support of this, we and others have previously shown that acute SIV infection in adult macaques causes rapid depletion of ILC3 in the GI tract (19, 20). Notably, HIV/SIV infection does not seem to directly cause depletion of ILC3 but instead alters the survival signals of ILCs, leading to a dramatic increase in apoptosis (21). Interestingly, ILC3 also undergo a functional shift during infection, moving from a tissue maintenance phenotype toward a proinflammatory profile with increased secretion of gamma interferon (IFN-γ), macrophage inflammatory protein 1 beta (MIP-1β), and tumor necrosis factor alpha (TNF-α) and decreased secretion of IL-17 and IL-22 (22, 23). Similarly, HIV/SIV viremia also induces functional and phenotypic changes in NK cells (9). Previous evidence indicated that lentiviral infection in pediatric populations actuated a reduction in cytotoxic function, as measured by the level of the degranulation marker CD107a, but an increase in the frequency of NK cells expressing activating receptors (24).

The use of nonhuman primates (NHP) in experimental infection studies has been paramount in studies of HIV/SIV (25). In an effort to better understand the mechanics of postnatal HIV transmission in human infants, members of our laboratory performed a comprehensive study of ILC3 and NK cells in SIV/SHIV-infected infant rhesus macaques (RM). The development of next-generation simian-human immunodeficiency viruses (SHIV) enables a more precise investigation of ontological differences in immune responses directed toward HIV between infants and adults. SHIV.C.CH505, a SHIV with enhanced CD4 binding and replication in RM, and SHIV-1157ipd3N4, an exclusively R5-tropic mucosally transmissible SHIV that induces high peak viral RNA loads, as well the traditionally used SIV_{mac251} strain, were chosen for this study as infection models (26, 27).

RESULTS

Infant RM lymphocyte frequencies in naive oral and GI mucosae. In an effort to further our understanding of innate immune responses to lentiviruses in infants, we performed the first comprehensive study of ILC3 and NK cells in a large cohort of infant RM. Using polychromatic flow cytometry, we evaluated the frequencies of cells in the colon and oral tissues, including tonsils, cervical lymph nodes (CLN), retropharyngeal lymph nodes (RLN), and submandibular/submental lymph nodes (SubLN), of SIV/SHIV-naive, healthy animals. To identify ILC3 and NK cells, we first gated on the lymphocyte population, followed by a single cell gate, and then LIVE/DEAD, and $CD45^+$ leukocytes to exclude debris and contaminating epithelial cells. Then, using our gating strategy, which was specifically designed for RM (HLA-DR^{dim} $CD3^-$ $CD14^-$), mononuclear cells were identified using NKG2A/C as a positive marker for NK cells and NKp44 for ILC3 (Fig. 1) (28). As expected, the colon had the highest frequency of ILC3 (Fig. 1B; see also Fig. 3A) (median percentage among $CD45^+$ mononuclear cells, 0.33%). This was approximately half a log higher than the level seen in the tonsil and over a log higher than that seen in the SubLN, CLN, and RLN (median frequencies, 0.087, 0.013, 0.0059, and 0.023%, respectively). NK cells were found in much higher frequencies in colon tissue (1.51%), again with a log to half-log decrease in oral tissues (Fig. 1B; see also Fig. 3B).

SIV/SHIV infection induces partial loss of ILC3 in the intestinal but not oral mucosae and induces systemic expansion of NK cells. Apart from flow cytometric analyses, we investigated the anatomical landscape of ILC *in situ* using a hybrid immunohistochemistry/*in situ* hybridization approach in both tonsil and colon (29). We were able to distinguish ILC from IL-17-producing T cells based on the absence of CD3 staining coupled with detection of RORc mRNA (Fig. 2). Tissue sections from uninfected infant RM tonsil (Fig. 2A) and colon (Fig. 2B) exhibited diverse immune cell phenotypes with regard to CD3 and IL-17. Importantly, we noted a paucity of IL-17-positive ($IL\text{-}17^+$) cells in SHIV/SIV-infected tonsil (Fig. 2C) and colon (Fig. 2D), suggesting that, as seen in previous findings (30, 31), Th17 and ILC3 were preferentially lost early in lentiviral infection.

Previously, our laboratory reported that the loss of ILC3 in adult RM during acute and chronic SIV infection is rapid and compartmentalized (23). In an attempt to discover

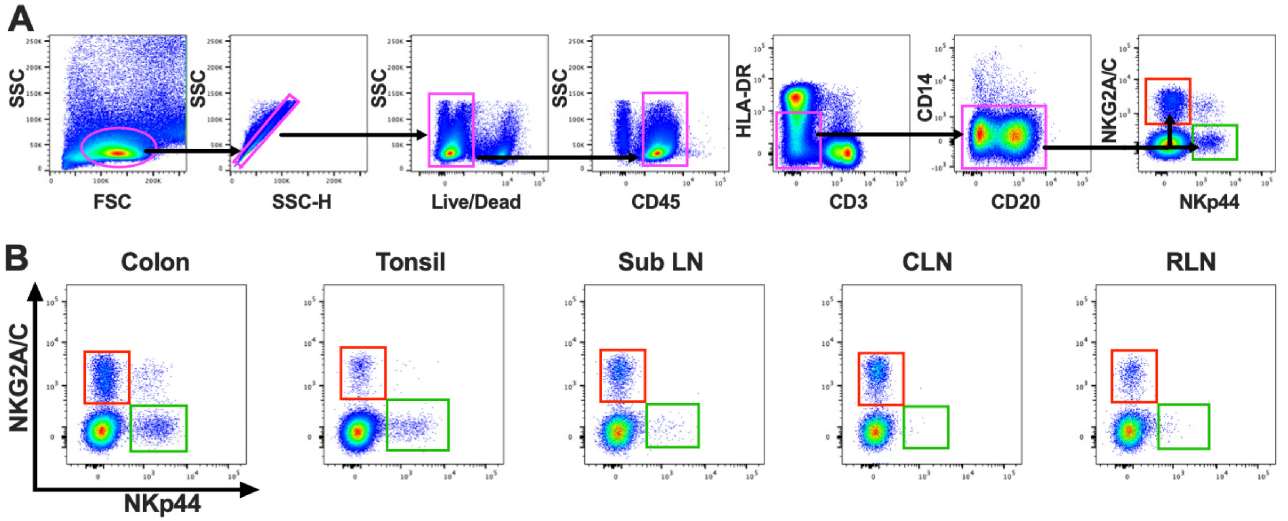

FIG 1 (A) Representative flow cytometry plots delineating identification of ILC3 (green box) and NK cells (red box) in infant RM. FSC, forward scatter; SSC, side scatter. (B) Anatomic distribution of NKG2A/C- and NKp44-expressing cell populations. Sub LN, submandibular/submental lymph nodes; CLN, cervical lymph nodes; RLN, retropharyngeal lymph nodes.

if this pathogenic progression also applies to pediatric infection, we orally infected infant RM to elucidate the effects of infection on the frequency and trafficking of ILC3 and NK cells in the oral mucosa (Fig. 3A and B) (Table 1). In support of preceding studies, we saw a nearly 3-fold decrease in the numbers of ILC3 in the colon after infection ($P = 0.0011$), a trend that was independent of the virus strain applied. This decrease was mirrored, albeit to a lesser extent, in the tonsils of infected animals, with a nearly 2-fold decrease in ILC3 populations. However, this loss did not reach statistical significance. Infection also induced a modest increase of ILC3 levels in the submental/submandibular and cervical lymph nodes (median frequencies, 0.027 and 0.034%, respectively), although this also did not reach statistical significance.

Median NK cell frequencies in the colon were lower in infected animals than in naive animals, but the differences did not reach statistical significance. However, NK cell frequencies were actually found to have increased in oral lymphoid tissues (Fig. 3B). In the tonsils and SubLN, we observed statistically significant and nearly statistically significant increases in the frequencies of NK cells and mononuclear cells, respectively ($P = 0.0439$ and 0.066).

To determine whether cellular influx or proliferation or both were responsible for the increased NK numbers, we assessed the trafficking repertoires and proliferation markers of ILC3 and NK cells in the colon and tonsils (Fig. 3 and 4). Although we detected a slight increase in Ki67 expression in ILC3, no such response was observed in NK cells (Fig. 3C to F), suggesting that the turnover rates were generally unaffected in these populations. One point of interest here, though, was that statistically significant differences in Ki67 expression between the RORγt bright and dim populations were observed only among the naive tonsil and colon samples ($P = 0.0286$) (Fig. 4E and F). No such differences were detected in the SHIV$^+$ samples. Consistent with our data representing acute SIV infection in adult RM, we did not detect an increase in the frequency of $\alpha 4\beta 7$, a gut-homing marker, but did in fact observe a trend of decreasing ILC3 expression in the colon upon infection ($P = 0.0571$). We then compared the trafficking markers CD62L and CD103 and also compared the chemokine receptors CCR5 and CXCR3. Here, we found no discernible change in the levels of CD103 expression except in colon NK cells ($P = 0.0571$). There did appear to be an overall trend of increased expression of CD62L and CXCR3 in the ILC3 and a slight curtailment of CXCR3 expression in the NK cells as a result of infection. Finally, multidimensional clustering indicated that the global phenotypic profiles of NK cells largely overlapped in colons and tonsils of naive and infected animals, but emergence of unique subsets

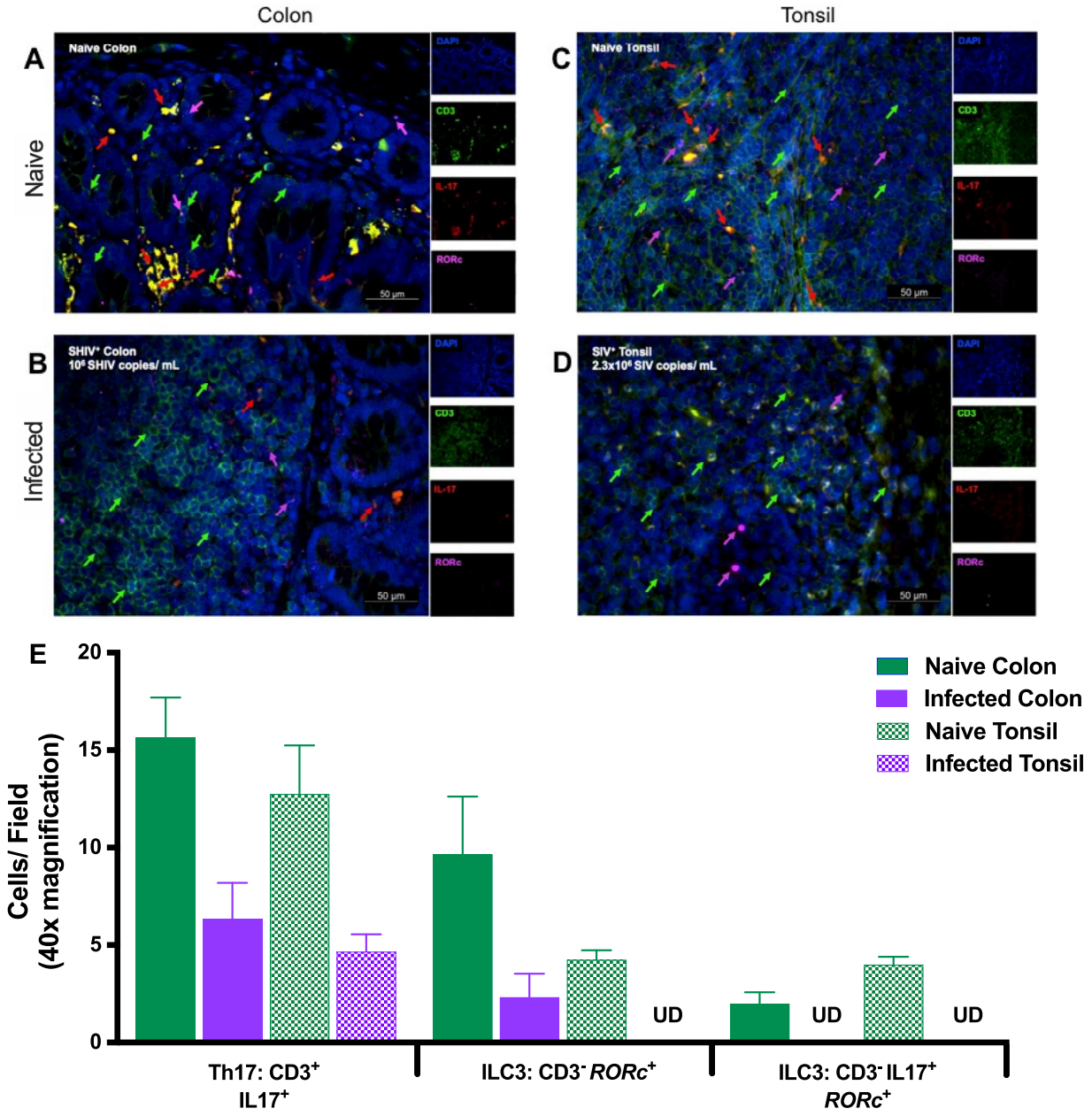

FIG 2 Immunohistochemistry analysis of infant rhesus macaque mucosae to detect ILC3 *in situ*. Sections were stained with the nuclear marker DAPI (4′,6-diamidino-2-phenylindole) (dark blue) and with antibodies specific for CD3 (green) and IL-17 (red). RORc mRNA, which encodes the RORγt protein, was detected by *in situ* hybridization (magenta). (A and B) Representative examples of tonsillar (A) and colon (B) tissues from naive infant macaques are shown. (C and D) Images of SIV_{mac251}-infected tonsil (C) and SHIV CH505 375H.dCT-infected colon (D) are also displayed. Individual channels are provided on the right. Arrow colors correspond to the indicated marker. The merged image has a scale bar in the lower right corner (imaged at ×40). (E) Enumerated cells from a minimum of three animals are displayed as cells per field. Solid green bars, naive colon; solid purple bars, SHIV-infected colon; hatched green bars, naive tonsil; hatched purple bars, SHIV-infected tonsil. Error bars represent means and standard errors. UD, undetectable in all fields.

indicative of increased cytotoxicity was observed, particularly in colon. Global phenotypes were also similar in colonic and tonsillar ILC3, where multidimensional clustering largely just confirmed the loss of cells during infection (Fig. 5).

ILC3 exhibit increased cytolytic activity in infected infant RM. After we identified ILC3 in tonsil, colon, and SubLN in naive and infected infant RM, we evaluated cell responses to mitogen stimulation in a multifunctional intracellular cytokine staining (ICS) assay. ILC3 displayed cytokine signatures that were distinct from those of NK cells (Fig. 6), and the differences were also compartmentalized by tissue (Fig. 7 and 8). In

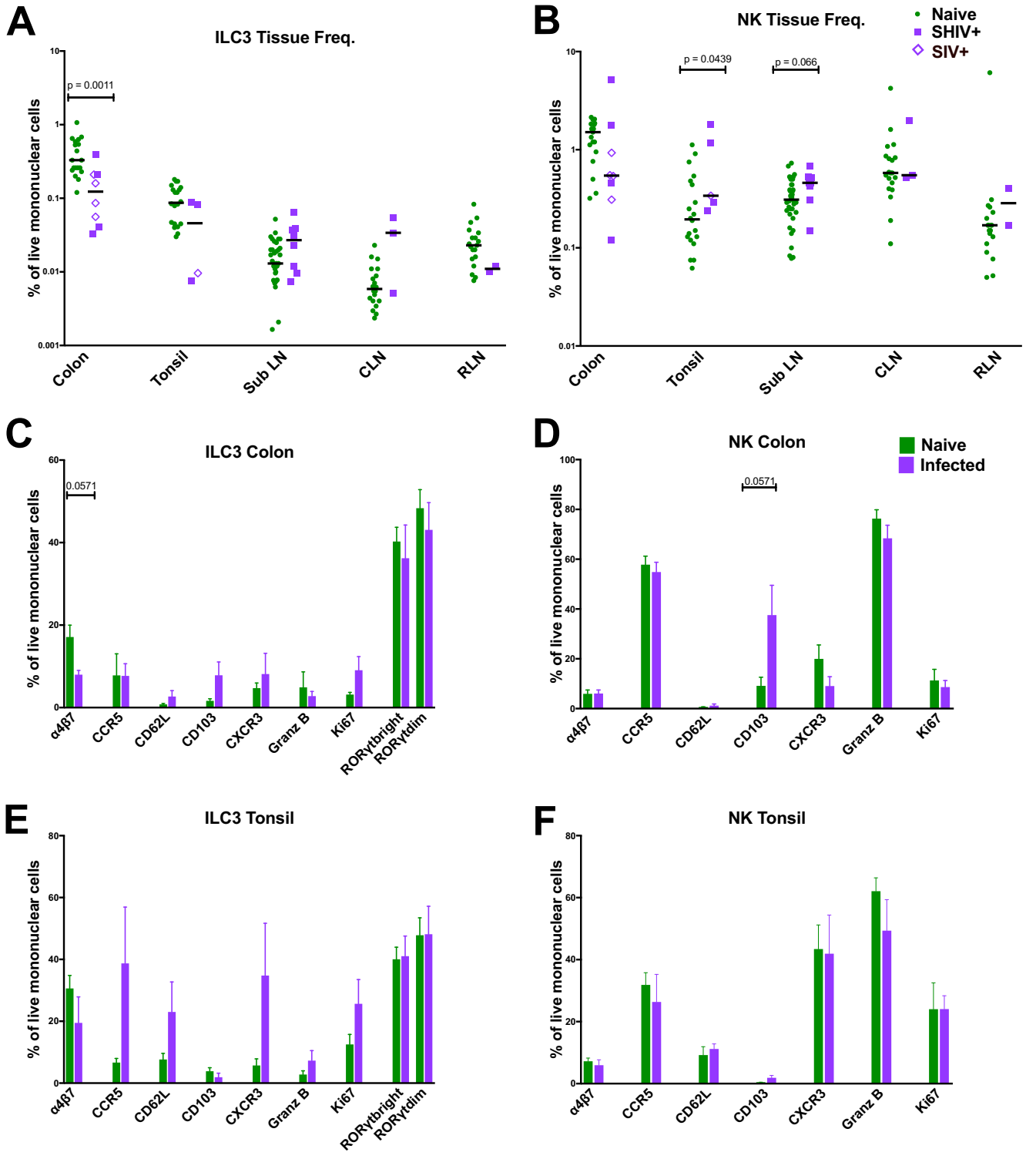

FIG 3 (A and B) Frequencies of ILC3 (A) and NK cells (B) among mononuclear cells in colon, tonsil, submandibular/submental lymph node (SubLN), cervical lymph node (CLN), and retropharyngeal lymph node (RLN) in naive and acutely SIV/SHIV-infected infant RM. (C to F) Percentages of ILC3 (C and E) and NK cells (D and F) in colon (C and D) and tonsil (E and F) tissue expressing trafficking, proliferating, and chemokine receptors compared between naive and acutely SHIV-infected macaques. Samples are from naive infant macaques ($n = 20$), those with SHIV infection ($n = 4$), and those with SIV infection ($n = 4$). The Mann Whitney U test was used to compare different quadrant populations. *, $P < 0.05$; **, $P < 0.01$; ***, $P < 0.005$.

TABLE 1 Summary of animals, viruses, and virologic outcomes

Study	Animal	Challenge virus	No. of challenges	Age at first exposure (wks)	Age at infection (wks)	Infection duration	Age at necropsy (wks)	Peak viremia (no. of copies/ml)	Necropsy viremia (no. of copies/ml)
1[a]	1A	SIVmac251	2	12	14	13	25	89,000,000	16,000,000
	1B	SIVmac251	10	12	22	12	24	48,000,000	900,000
	1C	SIVmac251	2	12	14	13	25	230,000,000	200,000,000
	1D	SIVmac251	1	12	13	13	25	16,000,000	1,700,000
	1E	SIVmac251	1	12	13	12	24	16,000,000	7,400,000
2[b]	2A	SHIV1157ipd3N4	18	12	30	6	18	210,000	4,600
	2B	SHIV1157ipd3N4	3	12	15	7	19	590,000	1,500
	2C	SHIV1157ipd3N4	3	12	14	8	20	26,000,000	910,000
	2D	SHIV1157ipd3N4	16	12	28	6	18	64,000,000	220,000
	2E	SHIV1157ipd3N4	1	12	12	7	19	33,000,000	58,000
	2F	SHIV1157ipd3N4	13	12	25	6	18	16,000	250
3	3A	SHIV.C.CH505.375H.dCT	2	6	8	27	36	4,700,000	18,000
	3B	SHIV.C.CH505.375H.dCT	2	6	8	27	35	2,800,000	1,300
	3C	SHIV.C.CH505.375H.dCT	17	6	23	23	42	1,000,000	1,000,000
	3D	SHIV.C.CH505.375H.dCT	2	6	8	25	35	2,900,000	20

[a]Data are from reference 44.
[b]Data are from reference 49.

general, ILC3 produced small amounts of CD107a and IFN-γ and produced MIP-1β intermittently. In contrast, ILC3 tended to produce the proinflammatory cytokine TNF-α and epithelial maintenance cytokines IL-17 and IL-22 (Fig. 7A). We found that ILC3 from the SubLN displayed profiles that were significantly different from those seen with ILC3 isolated from the colon ($P = 0.0486$) (Fig. 7C). ILC3 originating from the SubLN tended to produce more IL-22, MIP-1β, and TNF-α and less IL-17 than those originating from the colon. This functional difference was not seen between the LN and tonsils or between the tonsils and colon.

Next, we analyzed the effect that lentivirus infection had on the functional profile of ILC3 in the three tissues. Concurrent with previous findings from investigations performed in our laboratory in adult RM, we found that infection increased the proinflammatory and cytotoxic potential of ILC3 in both the tonsil and colon tissues but not in the oral lymph node tissues (Fig. 7B). We found a significant increase in the frequency of MIP-1β following SHIV infection in tonsil ILC3 ($P = 0.0121$). Although the data were not statistically significant, infection also induced an increase in CD107a, IFN-γ, and TNF-α expression in each tissue. SHIV infection caused a near-total loss of IL-22 production in both tonsillar and colon ILC3 ($P = 0.0364$ and $P = 0.0190$, respectively) but not in SubLN ILC3. Interestingly, this loss of function was not replicated with IL-17 production.

Compartmentalized perturbation of cytotoxic potential of NK cells in oral tissues. We investigated the functional profiles of NK cells following mitogen stimulation in SubLN, tonsil, and colon tissue. As expected, NK cells secreted little to no IL-17 and IL-22 and little TNF-α but did produce significant amounts of IFN-γ (Fig. 8A). Using multiparametric analysis, we found that the NK cells displayed compartmentalized functional profiles with highly significant differences between the SubLN and colon ($P = 0.0007$) and between the tonsil and colon ($P = 0.0305$) but not between the SubLN and tonsil (Fig. 8C). Naive SubLN NK samples produced copious amounts of MIP-1β, TNF-α, and IFN-γ. Although the quantities of IFN-γ secreted by the NK cells originating from colon tissue were similar to the quantities secreted by the NK cells originating from the SubLN, they favored a higher level of expression of CD107α, while expressing much less MIP-1β and TNF-α.

Finally, we tested the functionality of NK cells from SHIV$^+$ tonsil, colon, and SubLN. NK cytokine profile changes differed between tissues in response to SHIV infection (Fig. 8B). Curiously, NK functional perturbation was statistically significant only in SubLN with infection ($P = 0.0250$). Despite a lack of statistical significance in the results of compar-

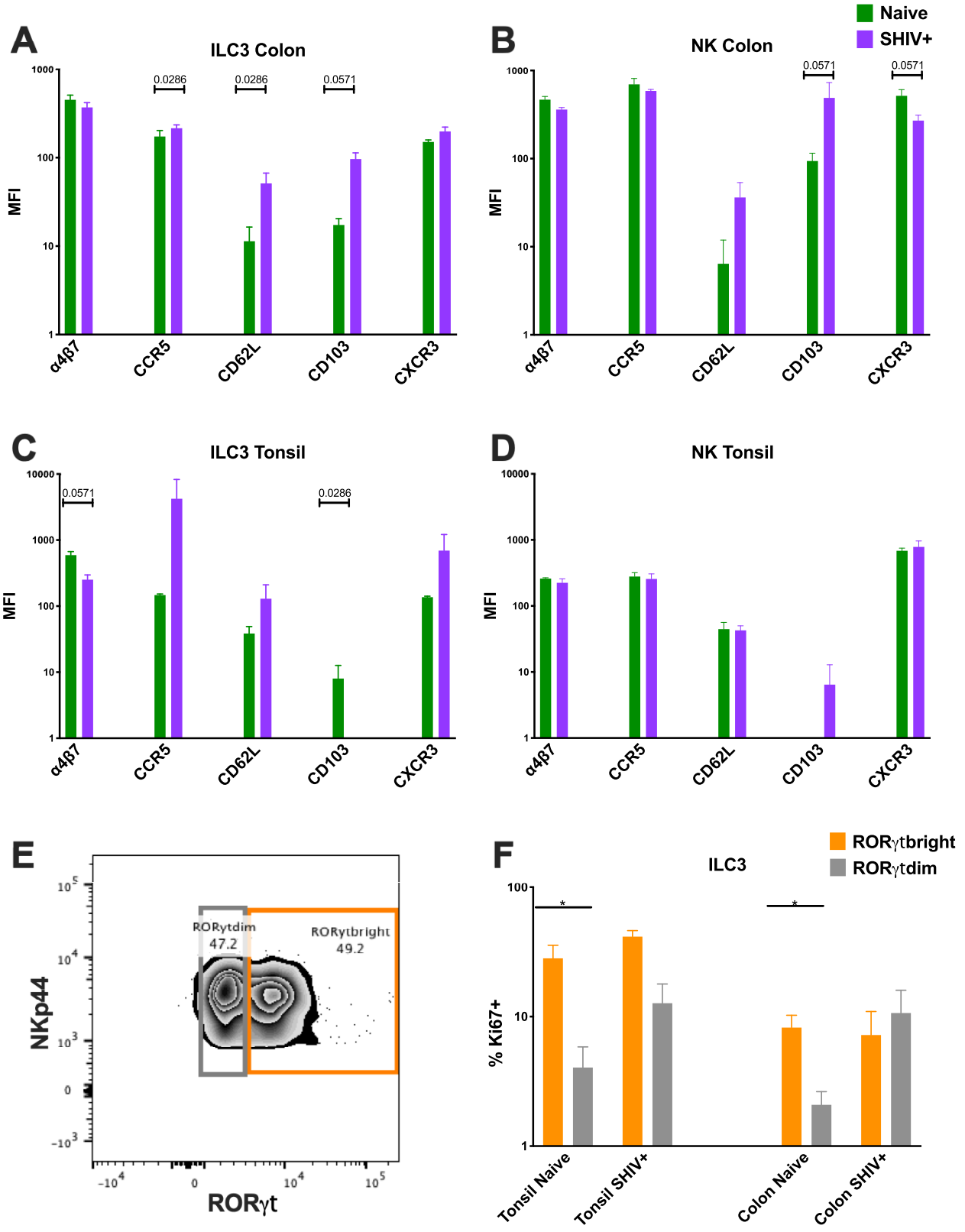

FIG 4 (A to D) Mean fluorescence intensity (MFI) plots of ILC3 (A and C) and NK (B and D) cells in colon (A and B) and tonsil (C and D) tissue expressing trafficking, proliferating, and chemokine receptors compared between naive and acutely SHIV-infected RM. Samples are from naive infant RM ($n = 4$) and from those with SHIV infection ($n = 4$). (E) Representative flow cytometry plot delineating RORγdim versus RORγtbright within the ILC3 population. (F) Percentages of Ki67-expressing ILC3 with bright versus dim RORγt expression. The Mann Whitney *U* test was used to compare different quadrant populations. *, $P < 0.05$; **, $P < 0.01$; ***, $P < 0.005$.

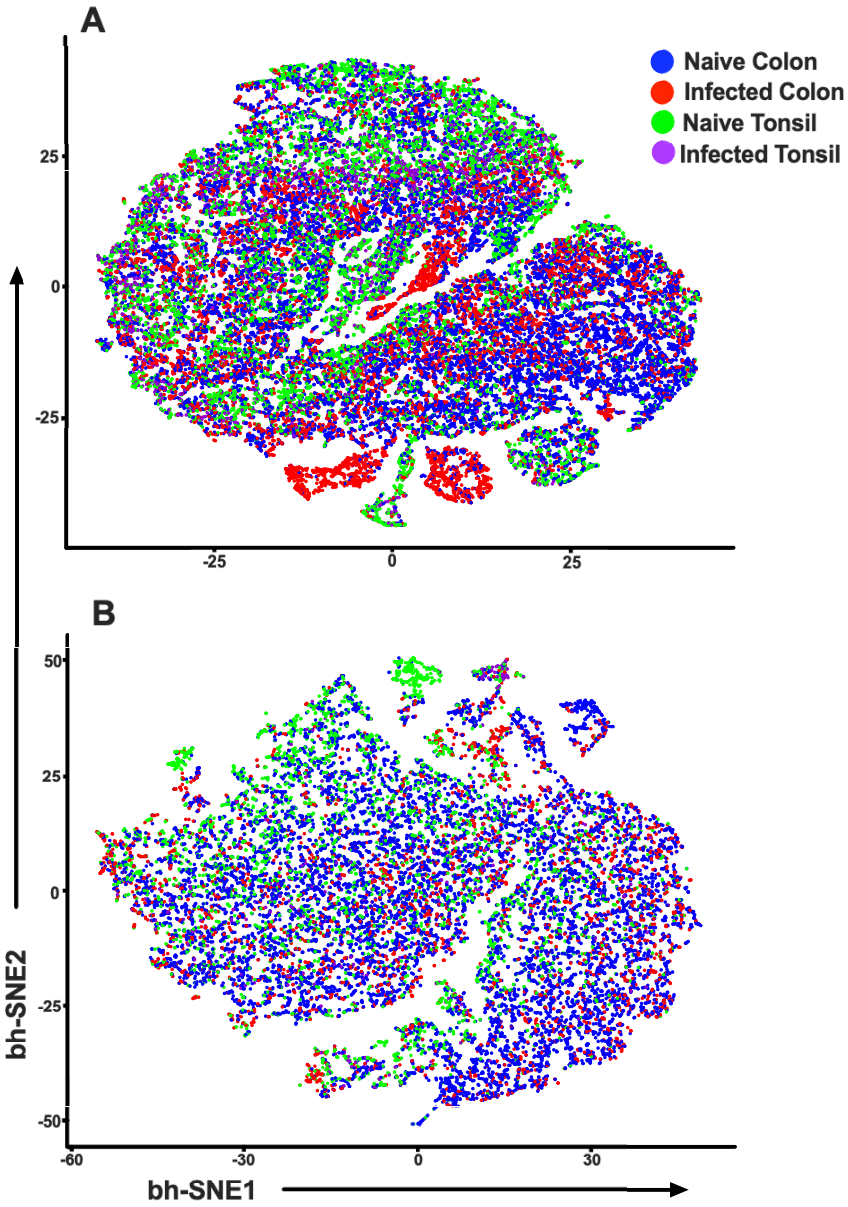

FIG 5 *t*-SNE plots indicating multidimensional analyses of NK cells (A) and ILC3 (B) using the phenotypic parameters described for Fig. 3.

isons between expression levels, analysis revealed a shift toward increased cytotoxic potential of NK cells in SHIV$^+$ animals, with trends toward higher levels of expression of CD107a, MIP-1β, and TNF-α.

DISCUSSION

To the best of our knowledge, this report presents the first comprehensive analysis of the impact of SIV/SHIV infection on ILC3 and NK cells in the oral mucosae and GI tissues of infant RM. We observed a substantial depletion of ILC3 in the colon of infected animals that contrasted with an expansion of both ILC3 and NK cells in various compartments of the oropharyngeal mucosae. This expansion can be partially explained by alterations to trafficking and chemokine receptors, specifically, CD62L, CD103, and CXCR3. Furthermore, we found that ILC3 and NK cells displayed tissue-specific functional repertoires that were perturbed by infection.

Previously, we reported that ILC3 were depleted in the colon during both acute and

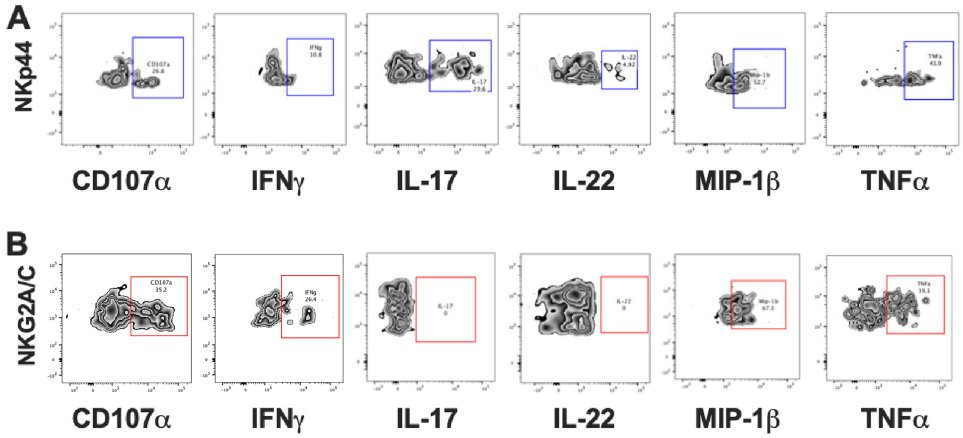

FIG 6 Flow cytometry plots depicting CD107a and intracellular cytokine responses in the 2 cell populations after mitogen stimulation. (A) ILC3. (B) NK cells. Gates were set based on unstimulated samples. Data from polychromatic flow cytometry and ICS experiments are representative of results from 3 to 8 animals per group.

chronic SIV infections of adult RM but that that response was followed by partial expansion in the oral mucosa (22, 23, 32). Since those initial findings were published, others have corroborated our results in the GI mucosae of SIV-infected RM and persons living with HIV (PLWH) (33, 34). Multiple analyses revealed that this loss was due in part to increased concentrations of local inflammatory cytokines (19, 20, 22). We saw similar results in orally infected infant RM; however, due to the limited sample availability typical of infant studies, we were unable to confirm whether the full mechanism found in adults was recapitulated (Fig. 3A). This expansion in select tissues in the oral mucosa can also be partially explained by alterations in trafficking and in the chemokine signature induced by infection. Although the data were not statistically significant, we saw specific increases in CD62L and CXCR3 expression. Increases in CXCR3 levels result in recruitment of a variety of immune cells to sites of inflammation, as it binds to the chemokine CXCL10. Both CXCR3 and CXCL10 are upregulated in HIV and SIV infections and may redirect ILC3 and NK cell migration and accumulation (35).

Since their initial description, the role of ILC3 in maintaining mucosal homeostasis and epithelial integrity has been repeatedly demonstrated (13, 14). Thus, it is important to understand how lentiviral infection impacts their capacity to fulfill those functions. Indeed, our data in infant RM support previous results reflecting this role, as we found that ILC3 from the SubLN, tonsil, and colon all produced significant amounts of IL-17 and IL-22, tissue-signaling cytokines that support protection and regeneration of the epithelial barrier and also protect the cells from opportunistic pathogens (36). Not surprisingly, infection abrogated ILC3 homeostatic functions, with results showing an antimicrobial functional profile, secretion of higher levels of MIP-1β, IFN-γ, and up-regulation of CD107a (Fig. 7A and B). Indeed, our data also revealed a systemic loss of IL-22 production, but not IL-17 production, by ILC3 in the tonsil and colon of infected RM. This disparity supports our finding of sustained RORγt expression in ILC3 during infection, as IL-17 expression is directly mediated by RORγt protein binding to IL-17 gene promoter and/or regulatory elements (37). Meanwhile, IL-22 expression is also dependent on the transcription factor AHR, whose ligands include environmental toxins and endogenous ligands, which indicates that SIV/SHIV infection might disrupt the microenvironment in which sampling of ILC3 occurred in specific tissues (38). Interestingly, and similarly to our findings in adult RM showing that ILC3 dysregulation is compartmentalized (22), ILC3 in the SubLN did not demonstrate this change in function.

In partial contrast to our previous findings in adult RM (22), we found a significant expansion of the NK cell population in the tonsil and SubLN in SHIV/SIV-infected infants (Fig. 3B). However, this increased magnitude did not appear to be associated with

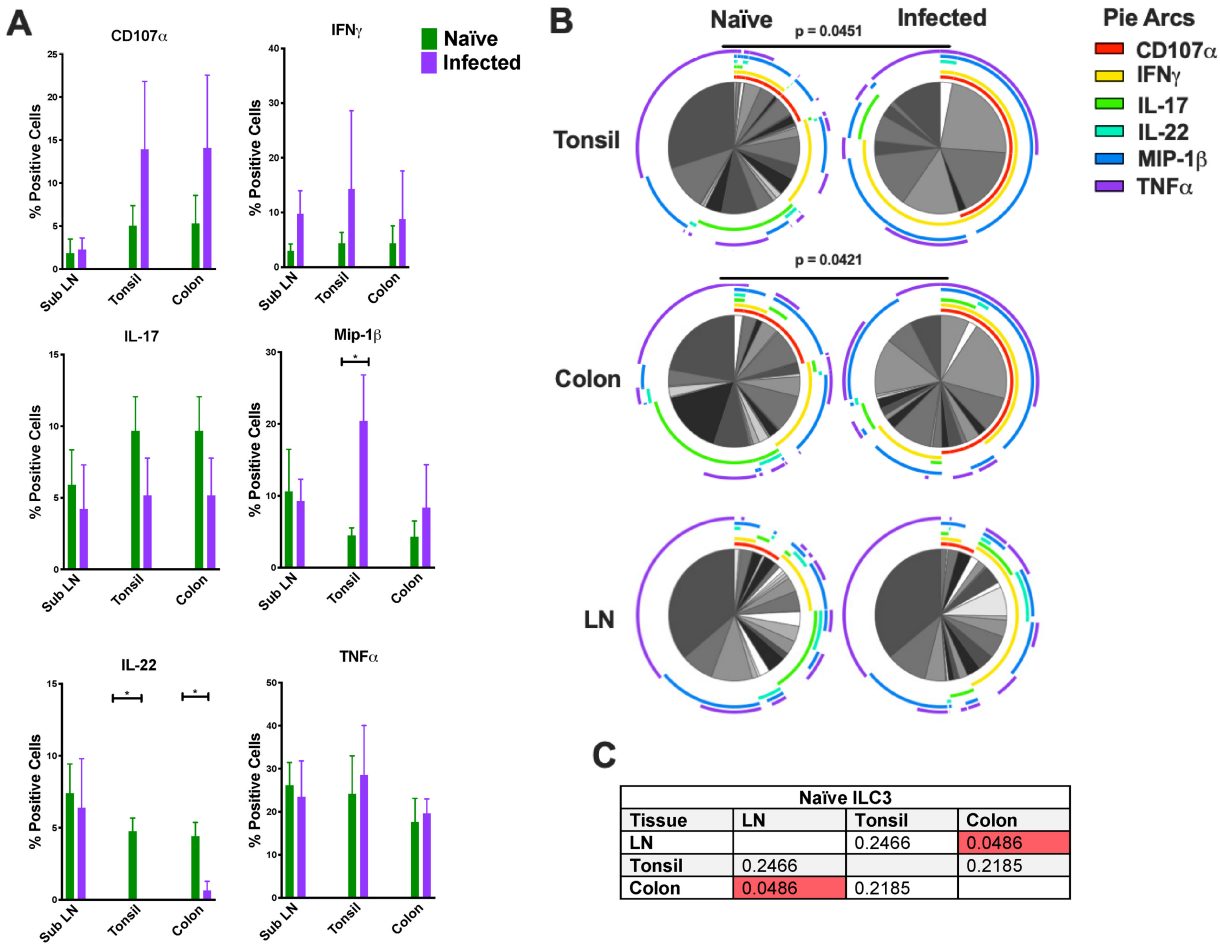

FIG 7 (A) Bar graphs depicting CD107a and intracellular cytokine responses in ILC3 following mitogen stimulation. (B) Multiparametric analyses of the data shown in panel A were performed using SPICE 6.0 software. Pies indicate means of results from 3 to 8 animals per group for each multifunction, and arcs show an overlap of individual functions (Naïve, SubLN $n = 6$, tonsil $n = 8$, and colon $n = 6$; Infected [SHIV$^+$], SubLN $n = 6$, tonsil $n = 3$, and colon $n = 4$). (C) *P* values for results of comparisons of naive ILC3 data performed using multiparametric SPICE analysis. The Mann Whitney *U* test was used to compare different quadrant populations. *, $P < 0.05$; **, $P < 0.01$; ***, $P < 0.005$.

protection as there was no relationship between NK cell frequencies in tissues and either peak viral load or viral load at necropsy (data not shown). Of note, this increased magnitude could have been a result of an altered trafficking repertoire, as an increase of CD103 expression has been shown previously to play an important role in the retention of NK cells and CTL in the oral mucosa (39, 40). Interestingly, Woodberry and colleagues had shown that CD103 expression was linked with a higher reactivity, corroborating earlier findings obtained in our laboratory indicating that infection increased frequencies of activating receptors on NK cells (22). Similarly to ILC3, NK cells from the SubLN, tonsil, and colon displayed compartmentalized functions. Colon NK cells exhibited a higher propensity for a cytotoxic phenotype than those from the oral mucosa, and that propensity was maintained during infection, although NK cells from all tissues exhibited a competent four-function response (TNF-α, IFN-γ, MIP-1β, and CD107a) (Fig. 8A and B).

In summary, our study revealed that acute SIV/SHIV infection has significant effects on the frequency, phenotype, and function of innate cells in the oral and gut mucosa. As ILC3 and NK cells are critical populations in the protection and maintenance of the oral mucosa, understanding how lentiviral infection perturbs their functional niches can provide a better understanding of how opportunistic diseases/coinfections may exploit these changes the oral mucosae during HIV infection. This is particularly relevant in infants infected with HIV, where the immune system is not fully functional and the

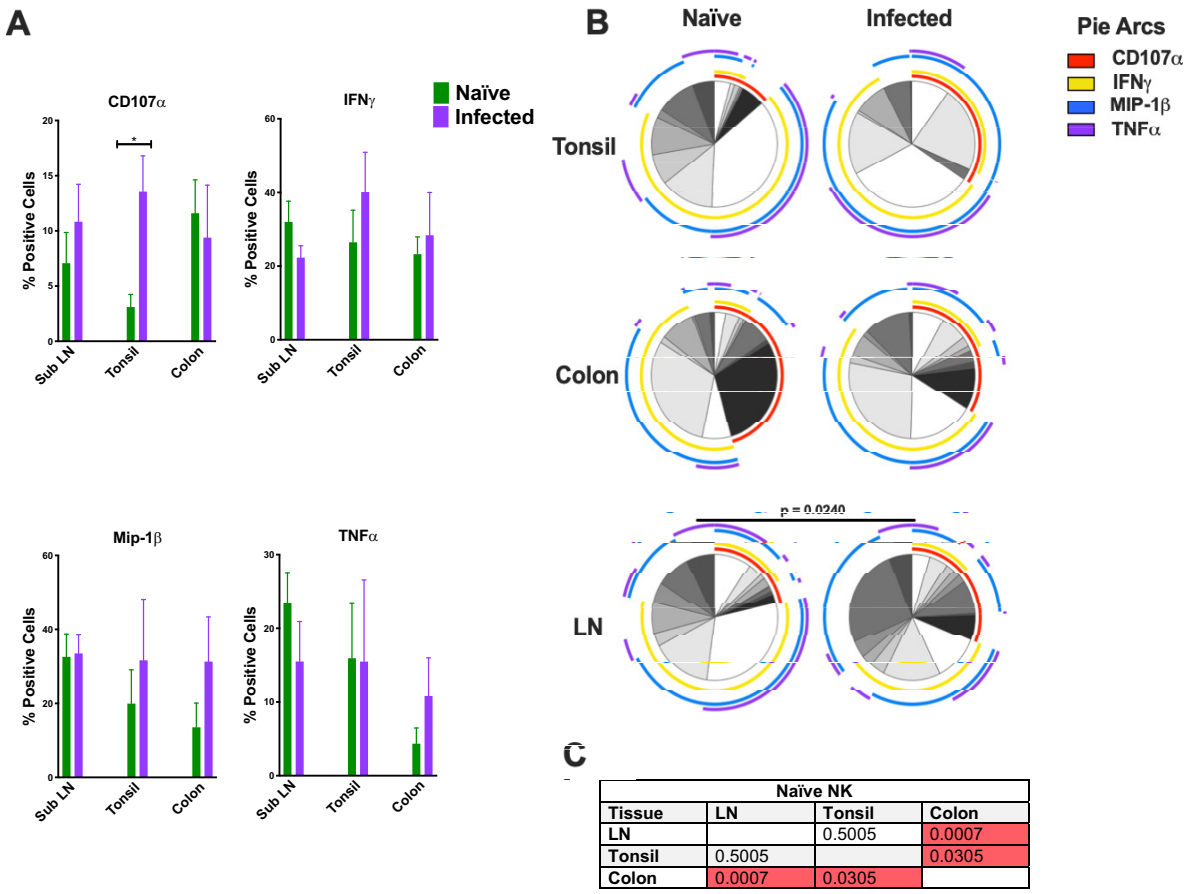

FIG 8 (A) Bar graphs depicting CD107a and intracellular cytokine responses in NK cells following mitogen stimulation. (B) Multiparametric analyses of the data shown in panel A were performed using SPICE 6.0 software. Pies indicate means of results from 3 to 8 animals per group for each multifunction, and arcs show an overlap of individual functions (Naïve, SubLN $n = 8$, tonsil $n = 8$; and colon $n = 6$; Infected [SHIV$^+$], SubLN $n = 8$, tonsil $n = 3$, and colon $n = 6$). (C) *P* values for results of comparisons of naive NK cell data performed using multiparametric SPICE analysis. The Mann Whitney *U* test was used to compare different quadrant populations. *, $P < 0.05$; **, $P < 0.01$; ***, $P < 0.005$.

effects are further compounded by the presence of the virus itself. Whether this is attributable to an altered microbiome, chronic inflammation, or some other mechanism is underdetermined and warrants further study into the underlying consequences of oral innate perturbation and its clinical significance.

MATERIALS AND METHODS

Animals and SHIV/SIV infections. This study utilized samples from previous studies, and no animals were acquired specifically for the analyses described here. The animals were housed and all experimental procedures were performed at the California National Primate Research Center (CNPRC), a facility accredited by the Association for Assessment and Accreditation of Laboratory Animal Care International (AAALAC). All animal care was performed in compliance with the Guide for the Care and Use of Laboratory Animals provided by the Institute for Laboratory Animal Research (2011) and the Weatherall report entitled "The use of nonhuman primates in research." The studies were approved by the Institutional Animal Care and Use Committee of the University of California, Davis (protocols 18650, 18655, and 19779). The macaques were kept in indoor housing in stainless steel cages (Lab Product, Inc.), were exposed to a 12-h light/12-h dark cycle (65 to 75°F, 30% to 70% room humidity), and received enrichment. Animals had free access to water and initially received infant formula; the infant formula was gradually replaced with commercial chow (high protein diet; Ralston Purina Co.) and fresh fruit and vegetable supplements. When necessary, macaques were immobilized with ketamine HCl (Parke-Davis) at approximately 10 mg/kg of body weight and injected intramuscularly after overnight fasting. Blood samples were collected using venipuncture. Animals were euthanized with an overdose of pentobarbital, followed by necropsy with extensive tissue collection.

A total of 35 rhesus macaques (*Macaca mulatta*) were analyzed in this study, including 20 naive animals, 4 SHIV.C.CH505.375H.dCT-infected animals, 6 SHIV1157ipd3N4-infected animals, and 5 SIVmac251-infected animals. The animals were of Indian origin and from the type D retrovirus-free, SIV-free, and STLV-1-free colony of the California National Primate Center (CNPRC; Davis, CA). Animals

were kept under conditions that complied with American Association for Accreditation of Laboratory Animal Care standards and the Guide for the Care and Use of Laboratory Animals (41).

The generation of SHIV.C.CH505.375H.dCT and SHIV1157ipd3N4 was previously described (27, 42). SHIV.C.CH505.375H.dCT and SHIV1157ipd3N4 challenge stocks (provided by George M. Shaw, University of Pennsylvania, and Ruth Ruprecht, Southwest National Primate Research Center, respectively) and SIV_{mac251} were used to orally challenge infant macaques. A summary of animals, viruses, and virologic outcomes in this study is provided as Table 1. All animals were euthanized at between 18 and 42 weeks of age. Tissues were collected from colon, tonsil, and submandibular, submental, cervical, and retropharyngeal lymph nodes.

Tissue processing. Processing of tissues was carried out using protocols optimized in our laboratory (28, 32, 43). Briefly, colon tissue was cut into 1-cm^2 sections and then incubated in 5 mM EDTA for 30 min before undergoing mechanical and enzymatic disruption. Samples were then gently pushed through filters before lymphocytes were isolated via the use of a bilayer (35%/60%) isotonic Percoll density gradient. Oral lymph nodes were trimmed of excess tissue and then mechanically disrupted. Manual cell counts were performed for each sample using trypan blue. Two million cells from each sample were then used for real-time flow cytometry staining, and the remaining cells were cryopreserved in a dimethyl sulfoxide (DMSO) solution and stored in liquid nitrogen vapor.

Antibodies and flow cytometry. Flow cytometry staining of mononuclear cells was carried out for cell surface molecules (see Table S1 in the supplemental material). Briefly, thawed samples were incubated with LIVE/DEAD Aqua amine dye (Invitrogen, Carlsbad, CA) and were then washed before staining with surface antibodies was performed. After staining, the cells were permeabilized using a Thermo Fisher Scientific Fix & Perm buffer kit (Thermo Fisher Scientific, Waltham, MA) and incubated with the intracellular staining antibodies. Isotype-matched controls were included in all assays. All acquisitions were made on an LSR II flow cytometer (BD Biosciences) and analyzed using FlowJo (10.5.3). Intracellular expression of the transcription factor RORγt was evaluated using the FoxP3 buffer set protocol (BD, Bedford, MA).

Stimulation assay. We analyzed multiple functions of ILC3 and NK cells *ex vivo* following mitogen stimulation (cell activation cocktail; BioLegend, San Diego, CA). Mononuclear cells were stimulated with cell activation cocktail, and anti-CD107a, GolgiPlug (brefeldin A) (Becton, Dickinson, Franklin Lakes, NJ), and GolgiStop (monensin) (Becton, Dickinson) were added directly into each of the tubes; unstimulated samples served as controls. All samples were then cultured for 12 h at 37°C in 5% CO_2. After incubation, samples were stained for surface and intracellular markers to delineate cell phenotype and function. The percentage of positive cells was calculated by subtracting the baseline cytokine expression in control samples.

Immunofluorescence assay. Tissue sections (5 μm) were seqentially cut and stained for CD3 and IL-17 as previously described (44). *In situ* hybridization was used to detect RORc mRNA via the use of a 1-Plex ViewRNA ISH tissue assay kit and SIV_{mac251} or beta actin (positive control) ViewRNA probe sets and a ViewRNA chromogenic signal amplification kit (all from Thermo Fisher, Waltham, MA) (44, 45). The slides were imaged with a Zeiss AxioObserver microscope and an AxioCam MRm camera. Composite overlays of CD3/IL-17-stained slides with ISH slides were prepared using Zen Lite v2.3 software (Zeiss). Quantitative measurements were obtained using ImageJ software (https://imagej.net/) (46). Cells were assessed for CD3, IL-17, and RORc mRNA and enumerated by hand using the Cell Counter Plugin for ImageJ (K. De Vos; https://imagej.nih.gov/ij/plugins/cell-counter.html).

Viral load quantification. Following initial challenge, virological analysis of weekly plasma samples was performed using reverse transcription-PCR (RT-PCR) for SIV/SHIV RNA as previously described (47) but with manual RNA extraction due to limited volumes. The limit of detection was 15 copies/ml. Samples showing transient low viremia followed by SIV/SHIV RNA-negative time points were retested to confirm the initial PCR results. Data are reported as the number of SIV/SHIV RNA copy equivalents per milliliter of plasma.

Statistical analysis. Statistical analyses were carried out using Prism Version 7.0d (GraphPad Software) and SPICE Version 6.0 (48). Unpaired, nonparametric, Mann-Whitney *U* tests and permutation tests were used where indicated, and *P* values of <0.05 were assumed to be significant. *t*-SNE (*t*-distributed stochastic neighbor embedding) analysis was performed using CytoDRAV (https://github.com/ReevesLab/CytoDRAV).

SUPPLEMENTAL MATERIAL

Supplemental material is available online only.

SUPPLEMENTAL FILE 1, PDF file, 0.04 MB.

ACKNOWLEDGMENTS

This work was supported by National Institutes of Health grants R01 DE026327, R01 AI143457, and R01 AI120828 (all to R.K.R.); R01 DE022287 and P01 AI117915 (both to K.D.P.); T32 5108303 (to A.D.C. II); the Harvard Center for AIDS Research (grant P30 AI060354); and the UNC Center for AIDS Research (grant P30 AI050410). The nonhuman primate studies performed at the California National Primate Research Center were supported by grant P51OD011107.

REFERENCES

1. UNAIDS. 2017. Start Free Stay Free AIDS Free—2017 progress report. http://www.unaids.org/sites/default/files/media_asset/JC2923_SFSFAF_2017progressreport_en.pdf.
2. UNAIDS. 2018. UNAIDS data 2018. http://www.unaids.org/sites/default/files/media_asset/unaids-data-2018_en.pdf.
3. Kuhn L, Aldrovandi G. 2010. Survival and health benefits of breastfeeding versus artificial feeding in infants of HIV-infected women: developing versus developed world. Clin Perinatol 37:843–862, x. https://doi.org/10.1016/j.clp.2010.08.011.
4. Dutzan N, Konkel JE, Greenwell-Wild T, Moutsopoulos NM. 2016. Characterization of the human immune cell network at the gingival barrier. Mucosal Immunol 9:1163–1172. https://doi.org/10.1038/mi.2015.136.
5. Belkaid Y, Harrison OJ. 2017. Homeostatic immunity and the microbiota. Immunity 46:562. https://doi.org/10.1016/j.immuni.2017.04.008.
6. Challacombe S, Sweet S. 2002. Oral mucosal immunity and HIV infection: current status. Oral Dis 8:55–62. https://doi.org/10.1034/j.1601-0825.2002.00013.x.
7. Greenspan D, Greenspan JS. 1996. HIV-related oral disease. Lancet 348:729–733. https://doi.org/10.1016/S0140-6736(96)02308-2.
8. Guilmot A, Hermann E, Braud VM, Carlier Y, Truyens C. 2011. Natural killer cell responses to infections in early life. J Innate Immun 3:280–288. https://doi.org/10.1159/000323934.
9. Fauci AS, Mavilio D, Kottilil S. 2005. NK cells in HIV infection: paradigm for protection or targets for ambush. Nat Rev Immunol 5:835–843. https://doi.org/10.1038/nri1711.
10. Mahapatra S, Shearer WT, Minard CG, Mace E, Paul M, Orange JS. 5 February 2019, posting date. NK cells in treated HIV-infected children display altered phenotype and function. J Allergy Clin Immunol https://doi.org/10.1016/j.jaci.2018.11.052.
11. Slyker JA, Lohman-Payne B, John-Stewart GC, Dong T, Mbori-Ngacha D, Tapia K, Atzberger A, Taylor S, Rowland-Jones SL, Blish CA. 31 December 2012, posting date. The impact of HIV-1 infection and exposure on natural killer (NK) cell phenotype in kenyan infants during the first year of life. Front Immunol https://doi.org/10.3389/fimmu.2012.00399.
12. Simoni Y, Fehlings M, Kløverpris HN, McGovern N, Koo SL, Loh CY, Lim S, Kurioka A, Fergusson JR, Tang CL, Kam MH, Dennis K, Lim TKH, Fui ACY, Hoong CW, Chan JKY, Curotto de Lafaille M, Narayanan S, Baig S, Shabeer M, Toh SAES, Tan HKK, Anicete R, Tan EH, Takano A, Klenerman P, Leslie A, Tan DSW, Tan IB, Ginhoux F, Newell EW. 2017. Human innate lymphoid cell subsets possess tissue-type based heterogeneity in phenotype and frequency. Immunity 46:148–161. https://doi.org/10.1016/j.immuni.2016.11.005.
13. Withers DR, Hepworth MR. 16 October 2017, posting date. Group 3 innate lymphoid cells: communications hubs of the intestinal immune system. Front Immunol https://doi.org/10.3389/fimmu.2017.01298.
14. Branzk N, Gronke K, Diefenbach A. 2018. Innate lymphoid cells, mediators of tissue homeostasis, adaptation and disease tolerance. Immunol Rev 286:86–101. https://doi.org/10.1111/imr.12718.
15. Penny HA, Hodge SH, Hepworth MR. 2018. Orchestration of intestinal homeostasis and tolerance by group 3 innate lymphoid cells. Semin Immunopathol 40:357–370. https://doi.org/10.1007/s00281-018-0687-8.
16. Liang SC, Tan X-Y, Luxenberg DP, Karim R, Dunussi-Joannopoulos K, Collins M, Fouser LA. 2006. Interleukin (IL)-22 and IL-17 are coexpressed by Th17 cells and cooperatively enhance expression of antimicrobial peptides. J Exp Med 203:2271–2279. https://doi.org/10.1084/jem.20061308.
17. Zhang Z, Cheng L, Zhao J, Li G, Zhang L, Chen W, Nie W, Blanco JRN, Wang FS, Su L. 2015. Plasmacytoid dendritic cells promote HIV-1-induced group 3 innate lymphoid cell depletion. J Clin Invest 125:3692–3703. https://doi.org/10.1172/JCI82124.
18. Klatt NR, Estes JD, Sun X, Ortiz AM, Barber JS, Harris LD, Cervasi B, Yokomizo LK, Pan L, Vinton CL, Tabb B, Canary LA, Dang Q, Hirsch VM, Alter G, Belkaid Y, Lifson JD, Silvestri G, Milner JD, Paiardini M, Haddad EK, Brenchley JM. 2012. Loss of mucosal CD103 DCs and IL-17 and IL-22 lymphocytes is associated with mucosal damage in SIV infection. Mucosal Immunol 5:646–657. https://doi.org/10.1038/mi.2012.38.
19. Xu H, Wang X, Lackner AA, Veazey RS. 2015. Type 3 innate lymphoid cell depletion is mediated by TLRs in lymphoid tissues of simian immunodeficiency virus-infected macaques. FASEB J 29:5072–5080. https://doi.org/10.1096/fj.15-276477.
20. Mudd JC, Busman-Sahay K, DiNapoli SR, Lai S, Sheik V, Lisco A, Deleage C, Richardson B, Palesch DJ, Paiardini M, Cameron M, Sereti I, Reeves RK, Estes JD, Brenchley JM. 27 September 2018, posting date. Hallmarks of primate lentiviral immunodeficiency infection recapitulate loss of innate lymphoid cells. Nat Commun https://doi.org/10.1038/s41467-018-05528-3.
21. Shah SV, Manickam C, Ram DR, Reeves RK. 13 December 2017, posting date. Innate lymphoid cells in HIV/SIV infections. Front Immunol https://doi.org/10.3389/fimmu.2017.01818.
22. Li H, Reeves RK. 8 January 2013, posting date. Functional perturbation of classical natural killer and innate lymphoid cells in the oral mucosa during SIV infection. Front Immunol https://doi.org/10.3389/fimmu.2012.00417.
23. Li H, Richert-Spuhler LE, Evans TI, Gillis J, Connole M, Estes JD, Keele BF, Klatt NR, Reeves RK. 2014. Hypercytotoxicity and rapid loss of NKp44$^+$ innate lymphoid cells during acute SIV infection. PLoS Pathog 10:e1004551. https://doi.org/10.1371/journal.ppat.1004551.
24. Ballan WM, Vu B-AN, Long BR, Loo CP, Michaëlsson J, Barbour JD, Lanier LL, Wiznia AA, Abadi J, Fennelly GJ, Rosenberg MG, Nixon DF. 2007. Natural killer cells in perinatally HIV-1-infected children exhibit less degranulation compared to HIV-1-exposed uninfected children and their expression of KIR2DL3, NKG2C, and NKp46 correlates with disease severity. J Immunol 179:3362–3370. https://doi.org/10.4049/jimmunol.179.5.3362.
25. Manickam C, Shah SV, Nohara J, Ferrari G, Reeves RK. 2019. Monkeying around: using non-human primate models to study NK cell biology in HIV infections. Front Immunol 10:1124. https://doi.org/10.3389/fimmu.2019.01124.
26. Bar KJ, Coronado E, Hensley-McBain T, O'Connor MA, Osborn JM, Miller C, Gott TM, Wangari S, Iwayama N, Ahrens CY, Smedley J, Moats C, Lynch RM, Haddad EK, Haigwood NL, Fuller DH, Shaw GM, Klatt NR, Manuzak JA. 28 August 2019, posting date. Simian-human immunodeficiency virus SHIV.CH505 infection of rhesus macaques results in persistent viral replication and induces intestinal immunopathology. J Virol https://doi.org/10.1128/jvi.00372-19.
27. Song RJ, Chenine A-L, Rasmussen RA, Ruprecht CR, Mirshahidi S, Grisson RD, Xu W, Whitney JB, Goins LM, Ong H, Li P-L, Shai-Kobiler E, Wang T, McCann CM, Zhang H, Wood C, Kankasa C, Secor WE, McClure HM, Strobert E, Else JG, Ruprecht RM, 15 August 2006, posting date. Molecularly cloned SHIV-1157ipd3N4: a highly replication-competent, mucosally transmissible R5 simian-human immunodeficiency virus encoding HIV clade C env. J Virol https://doi.org/10.1128/jvi.00558-06.
28. Reeves RK, Gillis J, Wong FE, Yu Y, Connole M, Johnson RP. 2010. CD16- natural killer cells: enrichment in mucosal and secondary lymphoid tissues and altered function during chronic SIV infection. Blood 115:4439–4446. https://doi.org/10.1182/blood-2010-01-265595.
29. Goswami R, Nelson AN, Tu JJ, Dennis M, Feng L, Kumar A, Mangold J, Mangan RJ, Mattingly C, Curtis AD, II, Obregon-Perko V, Mavigner M, Pollara J, Shaw GM, Bar KJ, Chahroudi A, De Paris K, Chan CA, Van Rompay KK, Permar SR, Goswami CR, Paris DK, Rompay V. 2019. Analytical treatment interruption after short-term antiretroviral therapy in a postnatally simian-human immunodeficiency virus-infected infant rhesus macaque model. mBio 10:e01971-19. https://doi.org/10.1128/mBio.01971-19.
30. Kløverpris HN, Kazer SW, Mjösberg J, Mabuka JM, Wellmann A, Ndhlovu Z, Yadon MC, Nhamoyebonde S, Muenchhoff M, Simoni Y, Andersson F, Kuhn W, Garrett N, Burgers WA, Kamya P, Pretorius K, Dong K, Moodley A, Newell EW, Kasprowicz V, Abdool Karim SS, Goulder P, Shalek AK, Walker BD, Ndung'u T, Leslie A. 2016. Innate lymphoid cells are depleted irreversibly during acute HIV-1 infection in the absence of viral suppression. Immunity 44:391–405. https://doi.org/10.1016/j.immuni.2016.01.006.
31. Klatt NR, Brenchley JM. 2010. Th17 cell dynamics in HIV infection. Curr Opin HIV AIDS 5:135. https://doi.org/10.1097/COH.0b013e3283364846.
32. Reeves RK, Rajakumar PA, Evans TI, Connole M, Gillis J, Wong FE, Kuzmichev YV, Carville A, Johnson RP. 2011. Gut inflammation and indoleamine deoxygenase inhibit IL-17 production and promote cytotoxic potential in NKp44$^+$ mucosal NK cells during SIV infection. Blood 118:3321–3330. https://doi.org/10.1182/blood-2011-04-347260.
33. Xu H, Wang X, Liu DX, Moroney-Rasmussen T, Lackner AA, Veazey RS. 2010. IL-17-producing innate lymphoid cells are restricted to mucosal

tissues and are depleted in SIV-infected macaques. Mucosal Immunol 46:220–231.
34. Krämer B, Goeser F, Lutz P, Glässner A, Boesecke C, Schwarze-Zander C, Kaczmarek D, Nischalke HD, Branchi V, Manekeller S, Hüneburg R, van Bremen T, Weismüller T, Strassburg CP, Rockstroh JK, Spengler U, Nattermann J. 2017. Compartment-specific distribution of human intestinal innate lymphoid cells is altered in HIV patients under effective therapy. PLoS Pathog 13:e1006373. https://doi.org/10.1371/journal.ppat.1006373.
35. Mehla R, Guha D, Ayyavoo V. 2013. Chemokine deregulation in HIV infection: role of interferon gamma induced Th1-chemokine signaling. J Clin Cell Immunol https://doi.org/10.4172/2155-9899.S7-004.
36. Eyerich K, Dimartino V, Cavani A. 2017. IL-17 and IL-22 in immunity: driving protection and pathology. Eur J Immunol 47:607–614. https://doi.org/10.1002/eji.201646723.
37. Gao W, Wu Y, Tian Y, Ni B. 2015. Yin–yang regulation of RORγt protein complex in Th17 differentiation. Int Rev Immunol 34:295–304. https://doi.org/10.3109/08830185.2014.969423.
38. Ramirez J-M, Brembilla NC, Sorg O, Chicheportiche R, Matthes T, Dayer J-M, Saurat J-H, Roosnek E, Chizzolini C. 2010. Activation of the aryl hydrocarbon receptor reveals distinct requirements for IL-22 and IL-17 production by human T helper cells. Eur J Immunol 40:2450–2459. https://doi.org/10.1002/eji.201040461.
39. Woodberry T, Suscovich TJ, Henry LM, August M, Waring MT, Kaur A, Hess C, Kutok JL, Aster JC, Wang F, Scadden DT, Brander C. 2005. Alpha E beta 7 (CD103) expression identifies a highly active, tonsil-resident effector-memory CTL population. J Immunol 175:4355–4362. https://doi.org/10.4049/jimmunol.175.7.4355.
40. Melsen JE, Lugthart G, Lankester AC, Schilham MW. 2016. Human circulating and tissue-resident CD56(bright) natural killer cell populations. Front Immunol 7:262. https://doi.org/10.3389/fimmu.2016.00262.
41. National Research Council. 2011. Guide for the care and use of laboratory animals, 8th ed. National Academies Press, Washington, DC. https://doi.org/10.17226/12910.
42. Liao HX, Lynch R, Zhou T, Gao F, Munir Alam S, Boyd SD, Fire AZ, Roskin KM, Schramm CA, Zhang Z, Zhu J, Shapiro L, Mullikin JC, Gnanakaran S, Hraber P, Wiehe K, Kelsoe G, Yang G, Xia SM, Montefiori DC, Parks R, Lloyd KE, Scearce RM, Soderberg KA, Cohen M, Kamanga G, Louder MK, Tran LM, Chen Y, Cai F, Chen S, Moquin S, Du X, Gordon Joyce M, Srivatsan S, Zhang B, Zheng A, Shaw GM, Hahn BH, Kepler TB, Korber BTM, Kwong PD, Mascola JR, Haynes BF, Becker J, Benjamin B, Blakesley R, Bouffard G, Brooks S, et al. 2013. Co-evolution of a broadly neutralizing HIV-1 antibody and founder virus. Nature 496:469–476. https://doi.org/10.1038/nature12053.
43. Abdel-Motal UM, Gillis J, Manson K, Wyand M, Montefiori D, Stefano-Cole K, Montelaro RC, Altman JD, Johnson RP. 2005. Kinetics of expansion of SIV Gag-specific $CD8^+$ T lymphocytes following challenge of vaccinated macaques. Virology 333:226–238. https://doi.org/10.1016/j.virol.2004.12.030.
44. Curtis AD, Walter KA, Nabi R, Jensen K, Dwivedi A, Pollara J, Ferrari G, Van Rompay KKA, Amara RR, Kozlowski PA, De Paris K. 2019. Oral coadministration of an intramuscular DNA/modified vaccinia Ankara vaccine for simian immunodeficiency virus Is associated with better control of infection in orally exposed infant macaques. AIDS Res Hum Retroviruses 35:310–325. https://doi.org/10.1089/AID.2018.0180.
45. Amedee AM, Phillips B, Jensen K, Robichaux S, Lacour N, Burke M, Piatak M, Lifson JD, Kozlowski PA, Van Rompay KKA, De Paris K. 1 March 2018, posting date. Early sites of virus replication after oral SIV_{mac251} infection of infant macaques: implications for pathogenesis. AIDS Res Hum Retroviruses https://doi.org/10.1089/aid.2017.0169.
46. Schneider CA, Rasband WS, Eliceiri KW. 2012. NIH Image to ImageJ: 25 years of image analysis. Nat Methods 9:671–675. https://doi.org/10.1038/nmeth.2089.
47. Nichole Cline A, Bess JW, Piatak MJ, Lifson JD. 2005. Highly sensitive SIV plasma viral load assay: practical considerations, realistic performance expectations, and application to reverse engineering of vaccines for AIDS. J Med Primatol 34:303–312. https://doi.org/10.1111/j.1600-0684.2005.00128.x.
48. Roederer M, Nozzi JL, Nason MC. 2011. SPICE: exploration and analysis of post-cytometric complex multivariate datasets. Cytometry A 79:167–174. https://doi.org/10.1002/cyto.a.21015.
49. Phillips B, Fouda GG, Eudailey J, Pollara J, Curtis AD, II, Kunz E, Dennis M, Shen X, Bay C, Hudgens M, Pickup D, Alam SM, Ardeshir A, Kozlowski PA, Van Rompay KKA, Ferrari G, Moody MA, Permar S, De Paris K. 2011. Impact of poxvirus vector priming, protein coadministration, and vaccine intervals on HIV gp120 vaccine-elicited antibody magnitude and function in infant macaques. Clin Vaccine Immunol 24:e00231-17. https://doi.org/10.1128/CVI.00231-17.